Original Article

PHARMACOPHORE MODELING AND ATOM-BASED 3D-QSAR STUDIES OF ANTIFUNGAL BENZOFURANS

SANDEEP S. PATHARE, SUJIT G. BHANSALI, KAKASAHEB R. MAHADIK, VITHAL M. KULKARNI*

Department of Pharmaceutical Chemistry, Poona College of Pharmacy, Bharati Vidyapeeth University, Erandwane, Pune 411038, Maharashtra, India.
Email: vmkulkarni60@gmail.com

ABSTRACT

Objective: To find out the common structural requirement which may be responsible for biological activity of benzofurans as potent N-myristoyltransferase (Nmt) inhibitors by the generation of ligand based pharmacophore hypothesis and atom-based 3D-QSAR model.

Methods: A set of 29 compounds were taken from the literature with their *in vitro* Nmt inhibitory data. A training set of 24 molecules and a set of five molecules was arbitrarily set aside as the test set. To generate 3D-QSAR models, training set was used and to validate the quality of the model, test set was used. A five-point pharmacophore model has been developed with two hydrogen bond acceptors (AA), one positive ionic atom (P) and two aromatic ring residues (RR). This is denoted as AAPRR.

Results: A statistically significant 3D-QSAR model for training set of 24 compounds was obtained using pharmacophore hypothesis AAPRR, with correlation coefficient ($r^2 = 0.916$) and high Fisher ratio (F =113.9). Also, the predictive power of generated model for test set of 5 compounds was found to be significant which was confirmed by the high value of cross validated correlation coefficient ($q^2 = 0.804$) and Pearson-R (0.917).

Conclusion: The results of ligand based pharmacophore hypothesis and atom based 3D-QSAR model explore the detailed structural perceptivities and also highlight the important binding features of benzofurans with Nmt.

Keywords: Phase, Pharmacophore, Atom based 3D-QSAR, Nmt Inhibitors.

INTRODUCTION

Fungal infections have increased dramatically in recent years. Life threatening infections caused by pathogenic fungi are becoming increasingly common, especially in those individuals with immune compromised hosts, such as patients undergoing anticancer chemotherapy or organ transplants and patients with AIDS [1]. Clinically, candidosis, aspergillosis and cryptococcosisare are three major fungal infections in immune compromised individuals [2, 3].

Currently available antifungal drugs for such infections essentially have three molecular targets: cytochrome P-450-dependent lanosterol 14α-demethylase, ergosterol, and 1,3-betaglucan synthase. The first is a fungistatic target vulnerable to resistance development; the second, while a fungicidal target, is not sufficiently different from the host to ensure high selectivity; and the third, a fungistatic (Aspergillus) or fungicidal (Candida) target, has limited activity spectrum and potential host toxicity that might preclude dose escalation. However, their use can suffer from limited efficiency, narrow antifungal spectrum, drug related toxicity, severer drug resistance, non- optimal pharmacokinetics and serious drug-drug interactions. Therefore, there is an emergent need to develop novel fungicidal drugs with a new mode of action.

Myristoyl-CoA: protein N-myristoyltransferase (Nmt; EC 2.1.3.97) is a cytosolic monomeric enzyme that catalyzes the transfer of the cellular fatty acid myristate (C14.0) from myristoyl- CoA to the N-terminal glycine amine of a variety of eukaryotic proteins [4]. Genetic studies have established that Nmt is essential for vegetative growth and survival of pathogenic fungi such as *Saccharomyces cerevisiae*. Nmt has also been proven to be essential for the viability of fungi, including the medically important Candida albicans (C. albicans) and Cryptococcus neoformans [5, 6].

Human Nmt has also been cloned and characterized. C. albicans Nmt has 451 amino acid residues, with a sequence identity of 45% to the human Nmt enzyme. Clear difference in the peptide–substrate specificity between fungal and human Nmts has been exploited, and Nmt has been identified as a potential chemotherapeutic target for

antifungal agents [7, 8]. Hence Nmt is an attractive target for the design and development of novel antifungal agents with a new mode of action without disrupting host Nmt. Because of its novel mechanism of action, Nmt inhibitors are expected to have advantages over azole antifungals in terms of activity against azole-resistant fungal strain and lack of drug–drug interactions, which are drawbacks of azole antifungal agents [9].

We have reported molecular modeling studies on various antifungal targets like cytochrome P-450-dependent lanosterol 14α-demethylase and squalene epoxidase [10, 11] for the rational design of new antifungal agents. Also, we have generated a 3D pharmacophore model using peptidic Nmt inhibitors and successfully utilized it for the design of nonpeptidic inhibitors [12, 13]. A novel series of benzofuran analogs was reported as nonpeptidic Nmt inhibitors [14-16]. Previously, we have reported 3D-QSAR on series of benzofuran analogs as antifungals using comparative molecular field analysis (CoMFA) [17] and Genetic function approximation (GFA) [18]. Our interest continues in benzofurans because of ease of synthesis of analogs.

Pharmacophore modeling has been one of the important and successful approach for new drug discovery since last few years. A pharmacophore model of the target binding site summarizes steric and electronic features needed for optimal interaction of a ligand with a target. Most common properties that are used to define pharmacophores are hydrogen bond acceptors, hydrogen bond donors, basic groups, acidic groups, partial charge, aliphatic hydrophobic moieties, and aromatic hydrophobic moieties. Pharmacophore features have been used extensively in drug discovery for virtual screening, *de novo* design, and lead optimization. A pharmacophore model of the target binding site can be used to virtually screen a compound library for putative hits. Apart from querying data base for active compounds, pharmacophore models can also be used by *de novo* design algorithms to guide the design of new compounds [19].

To continue our research efforts in the development of pharmacophore and 3D-QSAR of various therapeutic agents [20-22] we report here studies on pharmacophore generation and atom based

3D-QSAR model studies of a series of benzofurans using PHASE (Pharmacophore Alignment and Scoring Engine) [23] incorporated in Schrodinger Software, USA. The objective of the present study is to find out the common features which may be responsible for biological activity of benzofurans as potent N-myristoyl transferase inhibitors. The generated ligand based pharmacophore hypothesis and the cubes generated from atom-based 3D-QSAR model highlights the important structural features required for Nmt inhibition which can be useful further for design of potent N-myristoyl transferase inhibitors.

MATERIALS AND METHODS

Dataset

In the present study a set of 29 compounds were taken from the literature with their *in vitro* Nmt inhibitory data. [14-16] A training set of 24 molecules (molecules 1–24, table 1) were used to generate the QSAR models. The training set molecules were selected in such a way that they contained information in terms of both their structural features and biological activity ranges. The most active molecules, moderately active, and less active molecules were included, to spread out the range of activities [24]. To assess the predictive power of the model, a set of five molecules (molecules 24–29, table 1) was arbitrarily set aside as the test set. The test molecules were selected in such way that they truly represent the training set. To generate 3D-QSAR models, training set was used and to validate the quality of the model, test set was used. Biological activity used in the present study was expressed as:

$$pIC_{50} = -log_{10} \ IC_{50} \quad (1)$$

Where IC_{50} is the nanomolar concentration of the inhibitor producing 50% inhibition. In all the models subsequently developed, pIC_{50} values were used as the dependent variable. Structures and related inhibitory activities (IC_{50} values) are reported in table 1. Actual and predicted inhibitory activities (pIC_{50} values) and residual values are reported in table 1.

Table 1: Structure and activities of the molecules in the training (1–24) and test (25–29) sets
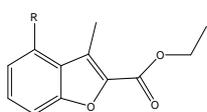
Comp.	R	Observed activity		Predicted activity	Residuals
		IC_{50} (µM)	pIC_{50} (Log1/IC_{50})	pIC_{50}	
1	$O(CH_2)_2NHC(CH_3)_3$	50	-1.698	-1.490	-0.208
2	$OCH_2CH(OH)CH_2NHCH(CH_3)_2$	0.98	0.008	0.08	-0.072
3	$O(CH_2)_3NHC(CH_3)_3$	1.7	-0.230	0.020	-0.250
4	$O(CH_2)_4NHC(CH_3)_3$	4.4	-0.643	-0.620	-0.023
5	$(H_2C)_3O$—N (piperidine)	1.6	-0.204	-0.070	-0.134
6	$O(CH_2)_5NHC(CH_3)_3$	15	-1.176	-1.470	0.294
25*	$O(CH_2)_2CH(OH)CH_2NHCH(CH_3)_2$	4.4	-0.643	-0.030	-0.613
26*	$O(CH_2)_2CH(OH)CH_2NHC(CH_3)_3$	1.2	-0.079	0.001	-0.080
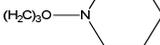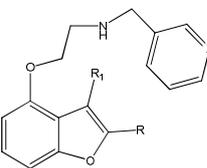
Comp.	R	R_1	X	Observed activity		Predicted activity	Residuals
				IC_{50} (µM)	pIC_{50} (Log1/IC_{50})	pIC_{50}	
7	CH_2CH_2Ph	CH_3	N	1.2	-0.079	-0.190	0.111
8	$CONHPh$	CH_3	N	2.2	-0.342	-0.250	0.092
9	CH_2SPh	CH_3	N	0.62	0.207	-0.030	0.237
10	$COOC_2H_5$	$c\text{-}C_3H_5$	N	4.4	-0.643	-0.520	-0.123
11	$COOC_2H_5$	CH3	CH	3.3	-0.518	-0.520	0.002
12	$COOC_2H_5$	CH_3	N	1	1.000	-0.380	1.380
21	$COOC_2H_5$	Et	N	10	-1.000	-0.650	-0.350
22	$COOC_2H_5$	i-propyl	N	83	-1.919	-1.520	-0.399
29*	$COOC_2H_5$	H	N	79	1.897	-1.532	3.429
23	(imidazole ketone)	CH_3	N	0.001	3.000	2.760	0.240
24	(benzofuran methylene ether)	CH_3	N	0.003	1.522	1.400	0.122
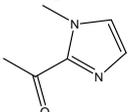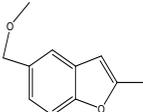
Ligand preparation

All molecules were built in Maestro and were prepared using Lig Prep [25] to convert 2D structure to 3D, generate stereoisomer, determine the most probable ionization state at user defined pH, neutralize charged structures, add hydrogen and to generate the possible number of energy minimized bioactive conformers using Conf Gen by applying OPLS-2005 force field [26]. Conformational space was explored through combination of Monte-Carlo Multiple Minimum (MCMM) / Low Mode (LMOD) with maximum number of conformers

1000 per structure and minimization steps 10000 [27, 28]. Each minimized conformer was filtered through a relative energy window of 50 kJ/mol and redundancy check of 2Å in the heavy atom positions.

Generation of Common Pharmacophore Hypothesis (CPH)

PHASE provides a standard set of six pharmacophoric features, hydrogen bond acceptor (A), hydrogen bond donor (D), hydrophobic group (H), negatively ionizable (N), positively ionizable (P), and aromatic ring (R) to define chemical feature of ligands. A five point common pharmacophore hypothesis (CPH) was identified from all the conformations of the active ligands having identical set of features with very similar spatial arrangement keeping minimum intersite distance of 2.0 Å.

Hypotheses were generated by a systematic variation of number of sites and the number of matching active compounds. CPH was considered, which indicated at least five sites common to all molecules.
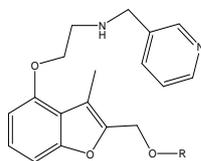
Compd	R	Observed activity		Predicted activity	Residuals
		IC$_{50}$ (µM)	pIC$_{50}$ (Log1/IC$_{50}$)	pIC$_{50}$	
13	2-Cynophenyl	0.017	1.769	2.070	-0.301
14	Phenyl	0.072	1.142	1.880	-0.738
15	3-Flurophenyl	0.11	0.958	1.640	-0.682
16	2,3-Diflurophenyl	0.0037	2.431	2.070	0.361
17	2-Flurophenyl	0.0083	2.080	1.970	0.110
18	2,3,4-Triflurophenyl	0.0057	2.244	2.130	0.114
19	2,4-Diflurophenyl	0.0075	2.124	2.030	0.094
20	4-Flurophenyl	0.0052	2.283	1.950	0.333
27*	4-Chlorophenyl	0.073	1.366	1.840	-0.474
28*	4-Cynophenyl	0.0094	2.026	1.480	0.546

* Test Set Compounds

Scoring pharmacophore hypothesis

Scoring procedure helps in ranking of the different hypotheses to yield the best alignment of the active ligands using an overall maximum root mean square deviation (RMSD) value of 1.2Å with default options for distance tolerance. Thus, it helps in making rational choice regarding which hypothesis is more appropriate for further investigation. The quality of alignment was measured by a survival score, [29, 30] defined as:

$$S = W_{site}S_{site} + W_{vec}S_{vec} + W_{vol}S_{vol} + W_{sel}S_{sel} + W^{m}_{rew} - W_{E}\Delta E + W_{act}A \quad ..(2)$$

where W's are weights and S's are scores; S_{site} represents alignment score, the RMSD in the site point position; S_{vec} represents vector score, and averages the cosine of the angles formed by corresponding pairs of vector features in aligned structures; represents volume score based on overlap of van der Waals models of non-hydrogen atoms in each pair of structures; and represents selectivity score, and accounts for what fraction of molecules are likely to match the hypothesis regardless of their activity toward the receptor. W_{site}, W_{vec}, W_{vol}, and W_{rew} have default values of 1.0, which has a default value of 0.0. In hypothesis generation, default values have been used. W_{sel} represents reward weights defined by m-1, where m is the number of actives that match the hypothesis. Hypotheses for which the reference ligand has a high energy relative to the lowest-energy conformer for that ligand are less likely to be good models of binding, because of the energetic cost hence a penalty for high-energy structures can be included by subtracting a multiple of the relative energy from the final score, $W_{E}\Delta E$. Similarly, for the hypothesis in which the reference ligand activity has relatively low energy than the highest activity can be penalized by adding a multiple of the reference ligand activity to the score, $W_{act}A$ where A is the activity [29, 30]. The generated hypothesis were scored and ranked to find out the best possible hypothesis. Further, the best CPH was selected depending on the adjusted survival score, until one hypothesis was found and scored successfully.

Building QSAR models

Pharmacophore based QSAR do not consider ligand features beyond the pharmacophore model, such as possible steric clashes with the receptor. This requires consideration of the entire molecular structure, so an atom-based QSAR model is more useful in explaining structure activity relationships. In atom-based QSAR, a molecule is treated as a set of overlapping Vander Waals spheres. Each feature is grouped according to a simple set of rules: hydrogen attached to polar atoms are classified as hydrogen bond donors (D); carbons, halogens, and C–H hydrogen are classified as hydrophobic/non-polar (H); atoms with an explicit negative ionic charge are classified as negative ionic (N); atoms with an explicit positive ionic charge are classified as positive ionic (P); non-ionic atoms are classified as electron-withdrawing (W); and all other types of atoms are classified as miscellaneous (X).

Validation of Pharmacophore Model

The main purpose to develop QSAR model was to predict biological activities of new compounds whereby the generated model will be statistically robust both internally as well as externally. The dataset was divided into training set and a test set. Atom-based 3D-QSAR models were generated for hypotheses using the 24 compounds in training set. The best QSAR model was externally validated by predicting activities of the 5 test set compounds.

The robustness of the developed pharmacophore hypotheses was internally validated by statistical parameters like squared correlation coefficient (r^2), q^2 (r^2 for test set), Standard deviation of regression (SD), Pearson correlation coefficient (Pearson-R), Statistical significance (P) and variance ratio (F). The predicted pIC$_{50}$ at 2nd PLS factor is given in table 3. Further increase in the number of PLS factors did not improve the statistics or predictive ability of the model [31, 32].

RESULTS AND DISCUSSION

Pharmacophore modeling and QSAR studies were performed using PHASE module of Schrodinger suite. The study is performed to generate 3D pharmacophoric features of benzofurans responsible for binding to target and to predict biological activity as N- myristoyl transferase inhibitors using atom based 3D-QSAR model.

Pharmacophore generation and 3D-QSAR model analysis

Common pharmacophore hypothesis (CPH) was developed using a set of 7 active ligands in "pharmset" as they contain important structural features crucial for binding to the receptor binding site.

We have used four minimum sites in find pharmacophore step and five maximum sites to generate optimum combination of features common to the most active compounds. The three and four featured pharmacophore hypothesis was rejected due to low value of survival score, as they were unable to define the complete binding space of the selected molecules. Five featured pharmacophore hypotheses were selected and subjected to stringent scoring function analysis.

CPH were generated with different combination of variants: AAPRR, AAHRR, AAARR, AARRR and 2455 CPH were generated with the variant AAPRR which was further considered for QSAR model generation and the results are given in table 2. Among the various generated pharmacophores, best hypothesis was identified by aligning the active compounds on hypothesis and calculating the survival score which helps in ranking all the hypotheses. The selected hypothesis distinguishes between the active and inactive molecules. Further, to confirm that the pharmacophore hypothesis maps with more active than inactive features, they were aligned to inactive compounds and scored. Hypothesis showing poor score were rejected. Therefore, adjusted survival score was calculated by subtracting the inactive score from survival score of this hypothesis (Table 2).
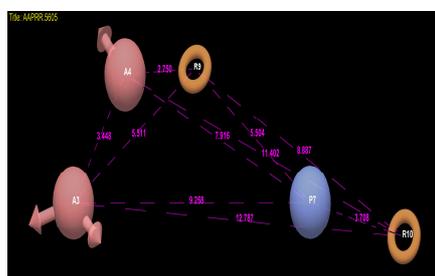

Fig. 1: Pharmacophore hypothesis and distance between pharmacophoric sites, all distances are in A^0 unit
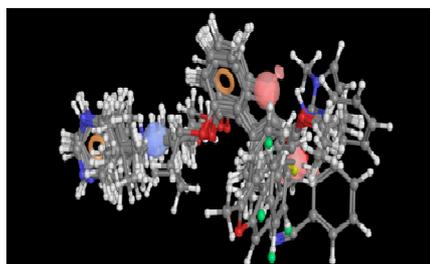

Fig. 2: Pharmacophore hypothesis AAPRR.5605 aligned on the all training set ligands
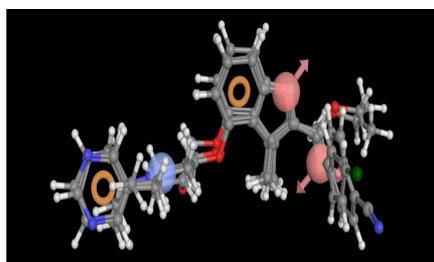

Fig. 3: Pharmacophore hypothesis AAPRR.5605 aligned on the all test set ligands

Finally the hypothesis with maximum adjusted survival score and lowest relative conformational energy was selected for generating atom-based 3D-QSAR model. The best model with good predictive power was found to be associated with the five points which consist of two hydrogen bond acceptor (AA), one positive ionic atom (P) and two ring feature (RR). This is denoted as AAPRR. The pharmacophore hypothesis showing distance between pharmacophoric sites is depicted in Fig. 1. As observed

in Fig. 2, among the two hydrogen bond acceptor groups(AA) one feature is mapped to 'O' of benzofuran ring, second one is observed on C=O attached to benzofuran ring. One positive ionic atom mapped to –NH group of side chain and two aromatic rings (RR) are present on benzene ring attached to side chain and in benzofuran ring.
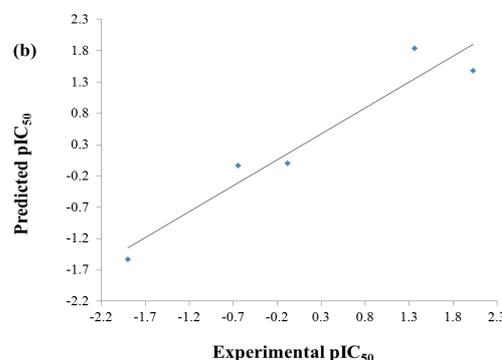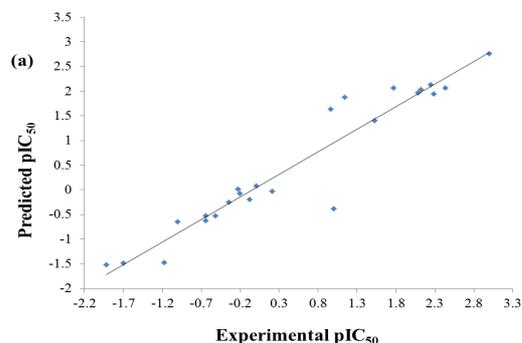

Fig. 4: Correlation graph of Experimental versus predicted pIC_{50} of training (a) and test sets (b)

The alignment generated by best pharmacophore hypothesis AAPRR is used for generation of 3D-QSAR model. From Fig. 2 and Fig. 3 it can be observed that active ligands have better alignment than inactive ligands.

Atom-based 3D-QSAR model was generated with 2nd PLS factor having good statistical significance and predictive power. PLS factor was increased up to two since up to second factor there is incremental increase in predictive power and statistical value of model.

A statistically significant 3D-QSAR model was obtained using this pharmacophore hypothesis with correlation coefficient value (r^2 = 0.916) and high Fisher ratio (F =113.9) for the training set of 24 compounds. Also, the predictive power of generated model was found to be significant which was confirmed by the high value of cross validated correlation coefficient (q^2 = 0.804) and Pearson-R (0.917) for the test set of 5 compounds.

The high value of F (113.9) indicates a statistically significant regression model, which is also supported by the low value of the variance ratio (P) indicating a high degree of confidence. The summary of atom based 3D-QSAR results is shown in table 3. Graphs of observed versus predicted biological activity of training and test set molecules are shown in fig. 4a and 4b respectively.

In order to visualize the generated 3D-QSAR model and to study its correlation with inhibitory activity one or more ligands from the series having diverse inhibitory activity were taken into consideration. The cubes were generated which represents important structural features required for interaction of ligand with active site of receptor which is shown in fig. 5 and 6 respectively for the most active and least active compounds in the series. In these

representations, the blue cubes indicate favorable regions while red cubes indicate unfavorable regions for biological activity. By using 3D-QSAR model the comparison was done to study favorable and unfavorable interaction using most active (compound 23) and least active (compound 22) as shown in Fig. 5 and 6 respectively.

On comparing fig. 5 and 6 it is observed that blue cubes are seen on C=O group and imidazole ring attached to benzofuran ring of compound 23 which suggest that highly polar groups are favored in this region. While, in compound 22 the imidazole ring is replaced by less polar ethoxy group and red cubes were seen in this region, which leads to tremendous decrease in the activity of compound 22.


Fig. 6: Visual representation of atom-based 3D-QSAR model on least active ligand 22

Fig. 5: Visual representation of atom-based 3D-QSAR model on most active ligand 23.

Hence, this suggests that more electronegative and polar groups are needed in this region and replacement with bulky groups will lead to decrease in activity. This is confirmed from the activities of compounds 13-20, 24, 27, and 28 which are having more polar and electronegative groups in this region hence they are active. While, the compounds 1-12, 21-22, 25-26, 29 have less polar and less electronegative groups, hence they are less active compounds. Also, blue cubes were observed around nitrogen and benzene ring which suggest that presence of nitrogen and aromatic residue is essential for activity which is revealed from the activities of compounds 13-20, 23-24 and 27-28.

Table 2: Best Pharmacophore hypothesis according to scoring values

S. No.	Hypothesis	Survival Active	Survival Inactive	Post-hoc Score	#Matches
1	AAPRR.6469	6.985	4.689	3.871	7
2	AAPRR.3639	6.931	4.604	3.933	7
3	AAPRR.946	6.919	4.553	3.937	7
4	AAPRR.5606	6.896	4.718	3.814	7
5	AAPRR.6467	6.881	4.676	3.779	7
6	AAPRR.5605	6.88	4.731	3.799	7
7	AAPRR.2729	6.87	4.539	3.933	7
8	AAPRR.2730	6.87	4.539	3.933	7
9	AAPRR.3633	6.862	4.655	3.836	7
10	AAPRR.3706	6.861	4.726	3.826	7

Table 3: Statistic parameters for best pharmacophore hypothesis

PLS Factors	SD	r^2	F	P	RMSE	q^2	Pearson-R
1	0.9058	0.6132	34.9	6.068e-006	0.5091	0.7752	0.9142
2	0.433	0.9156	113.9	5.313e-012	0.4758	0.8036	0.9168

CONCLUSION

A five point pharmacophore was generated by ligand based approach for benzofuran derivatives which reveals the importance of steric and electronic features of the ligand necessary for binding with target and responsible for activity. A highly predictive atom based 3D-QSAR model was generated using a training set of 24 molecules which consists of five point pharmacophore (AAPRR): two hydrogen bond acceptor (A), one positive ionic atom (P) and two aromatic ring feature (RR). Further, the developed model was visualized with cubes to identify the important structural features. It was observed that polar and electronegative groups attached to benzofurans ring are necessary for activity. Hence, the results of pharmacophore studies and atom based 3D-QSAR model shall further help in designing benzofurans analogues with better activity prior to synthesis and may show potent N-myristoyltransferase inhibition activity.

ACKNOWLEDGEMENT

The authors are grateful to Dr. Shivajirao S. Kadam, Vice Chancellor, Bharati Vidyapeeth University, Pune, Maharastra, India for providing the computational facility.

DISCLOSURE

The author reports no conflicts of interest in this work.

CONFLICT OF INTEREST

Declared None.

REFERENCES

1. Fridkin SK, Jarvis WR. Epidemiology of nosocomial fungal infections. Clin Microbiol Rev 1996;9:499-511.
2. Latge JP. Aspergillus fumigatus and aspergillosis. Clin Microbiol Rev 1999;12:310-50.
3. Steenbergen JN, Casadevall AJ. Prevalence of Cryptococcus neoformans var neoformans (Serotype D) and cryptococcus neoformans var grubii (Serotype A) isolates in New York City. Clin Microbiol 2000;38:1974-6.
4. Duronio RJ, Towler DA, Heuckeroth RO, Gordon JI. Disruption of the yeast N-myristoyl transferase gene causes recessive lethality. Sci 1989;243:796-800.
5. Weinberg RA, McWherter CA, Freeman SK, Wood DC, Gordon JI, Lee SC. Genetic studies reveal that myristoyl Co A: protein N-myristoyltransferase is an essential enzyme in Candida albicans. Mol Microbiol 1995;16:241-50.
6. Lodge JK, Machelski E, Toffaletti DL, Perfect JR, Gordon JI. Targeted gene replacement demonstrates that myristoyl-Co A: protein N-myristoyltransferase is essential for viability of Cryptococcus neoformans. Proc Natl Acad Sci USA 1994;91:12008-12.

7. Wilcox C, Hu JS, Olson EN. Acylation of proteins with myristic acid occurs cotranslationally. Sci 1987;238:275-8.
8. Johnson DR, Bhatnagar RS, Knoll LJ, Gordon JI. Genetic and biochemical studies of protein N-myristoylation. Annu Rev Biochem 1994;63:869-914.
9. Benedetti MS, Bani M. Metabolism-based drug interactions involving oral azole antifungals in humans. Drug Metab Rev 1999;31:665-717.
10. Talele TT, Kulkarni SS, Kulkarni VM. Development of pharmacophore alignment models as input for comparative molecular field analysis of a diverse set of azole antifungal agents. J Chem Inf Comput Sci 1999;39:958-66.
11. Gokhale VM, Kulkarni VM. Comparative molecular field analysis of fungal squalene epoxidase inhibitors. J Med Chem 1999;42:5348-58.
12. Karki RG, Kulkarni VM. A feature based Pharmacophore for Candida albicans MyristoylCoA: protein N-myristoyltransferase inhibitors. Eur J Med Chem 2001b;36:147-63.
13. Karki RG, Kulkarni VM. Computer-aided design and synthesis of Candida albicans N-myristoyltransferase inhibitors as antifungal agents. Indian Drugs 2001;38:406-13.
14. Masubuchi M, Ken-ichi K, Ebiike H, Ikeda Y, Tsujii S, Sogabe S, *et al*. Design and synthesis of novel benzofurans as a new class of antifungal agents targeting fungal N-myristoyltransferase Part 1. Bioorg Med Chem Lett 2001;11:1833-7.
15. Ebiike H, Masubuchi M, Liu P, Kawasaki K, Morikami K, Sogabe S, *et al*. Design and synthesis of novel benzofurans as a new class of antifungal agents targeting fungal N-myristoyltransferase Part 2. Bioorg Med Chem Lett 2002;12:607-10.
16. Ken-ichi K, Masubuchi M, Morikami K, Sogabe S, Aoyama T, Ebiike H, *et al*. Design and synthesis of novel benzofurans as a new class of antifungal agents targeting fungal N-myristoyltransferase Part 3. Bioorg Med Chem Lett 2003;13:87-91.
17. Purushottamachar P, Kulkarni VM. 3D-QSAR of N-myristoyltransferase inhibiting antifungal agents by CoMFA and CoMSIA methods. Bioorg Med Chem 2003;5:3487-97.
18. Deokar HS, Purushottamachar P, Kulkarni VM. QSAR analysis of N-myristoyltransferase inhibitors: antifungal activity of benzofurans. Med Chem Res 2009;18:206-20.
19. Yang SY. Pharmacophore modeling and applications in drug discovery: challenges and recent advances. Drug Discov Today 2010;15:444-50.
20. Bhansali SG, Kulkarni VM. Pharmacophore generation, atom-based 3D-QSAR, docking, and virtual screening studies of p38-α mitogen activated protein kinase inhibitors: pyridopyridazine-6-ones (part-2). Res Rep Med Chem 2014;4:1-21.
21. Bhansali SG, Kulkarni VM. 3D-QSAR of p38 mitogen activated protein kinase inhibitors: pyridopyridazine-6-ones (part-1). Res Rep Med Chem 2013;3:29-41.
22. Bhansali SG, Kulkarni VM. Combined 2D and 3D-QSAR, molecular modeling and docking studies of pyrazolodiazepinones as novel phosphodiesterase 2 inhibitors. SAR QSAR Environ Res 2014;25(11):905-37.
23. Phase, version 3.4, Schrödinger, LLC, New York NY; 2012.
24. Golbraikh A, Shen M, Xiao Z, Xiao Y, Lee K. Tropsha, A rational selection of training and test sets for the development of validated QSAR models. J Comput Aided Mol Des 2003;17:241-53.
25. Lig Prep, version 2.5, Schrödinger, LLC: New York NY; 2012.
26. Jorgensen WL, Maxwell DS, Tirado-Rives J. Development and testing of the OPLS all-atom force field on conformational energetic and properties of organic liquids. J Am Chem Soc 1996;118:11225-36.
27. Chang G, Guida WC, Still WC. An internal-coordinate monte carlo method for searching conformational space. J Am Chem Soc 1989;111:4379-86.
28. Kolossvary I, Guida WC. Low mode search. An efficient, automated computational method for conformational analysis: application to cyclic and acyclic alkanes and cyclic peptides. J Am Chem Soc 1996;118:5011-9.
29. Dixon SL, Smondyrev AM, Knoll EH, Rao SN, Shaw DE, Friesner RA. PHASE: a new engine for pharmacophore perception, 3D QSAR model development, and 3D database screening: 1. Methodology and preliminary results. J Comput Aided Mol Des 2006;20:647-71.
30. Dixon SL, Smondyrev AM, Rao S. Phase: a novel approach to pharmacophore modeling and 3d database searching. Chem Biol Drug Des 2006;67:370-2.
31. Shah UA, Deokar HS, Kadam SS, Kulkarni VM. Pharmacophore generation and atom-based 3D-QSAR of novel 2-(4-methylsulfonylphenyl) pyrimidines as COX-2 inhibitors. Mol Div 2010;14:559-68.
32. Teli MK. Pharmacophore generation and atom-based 3D-QSAR of N-iso-propyl pyrrole-based derivatives as HMG-CoA reductase inhibitors. Org Med Chem Lett 2012;2:25-34.